AMERICAN SOCIETY FOR MICROBIOLOGY | Applied and Environmental Microbiology®

MICROBIAL ECOLOGY

Vibrio fischeri Amidase Activity Is Required for Normal Cell Division, Motility, and Symbiotic Competence

Pat M. Fidopiastis,[a] Vanessa Mariscal,[a] Jeanne-Marie McPherson,[a] Sarah McAnulty,[b] Anne Dunn,[c] Eric V. Stabb,[d] Karen L. Visick[e]

[a]California State University, San Luis Obispo, California, USA
[b]University of Connecticut, Storrs, Connecticut, USA
[c]University of Oklahoma, Norman, Oklahoma, USA
[d]University of Illinois, Chicago, Illinois, USA
[e]Loyola University, Maywood, Illinois, USA

ABSTRACT *N*-Acetylmuramoyl-L-alanine amidases are periplasmic hydrolases that cleave the amide bond between *N*-acetylmuramic acid and alanine in peptidoglycan (PG). Unlike many Gram-negative bacteria that encode redundant periplasmic amidases, *Vibrio fischeri* appears to encode a single protein that is homologous to AmiB of *Vibrio cholerae*. We screened a *V. fischeri* transposon mutant library for strains altered in biofilm production and discovered a biofilm-overproducing strain with an insertion in *amiB* (*VF_2326*). Further characterization of biofilm enhancement suggested that this phenotype was due to the overproduction of cellulose, and it was dependent on the *bcsA* cellulose synthase. Additionally, the *amiB* mutant was nonmotile, perhaps due to defects in its ability to septate during division. The amidase mutant was unable to compete with the wild type for the colonization of *V. fischeri*'s symbiotic host, the squid *Euprymna scolopes*. In single-strain inoculations, host squid inoculated with the mutant eventually became colonized but with a much lower efficiency than in squid inoculated with the wild type. This observation was consistent with the pleiotropic effects of the *amiB* mutation and led us to speculate that motile suppressors of the *amiB* mutant were responsible for the partially restored colonization. In culture, motile suppressor mutants carried point mutations in a single gene (*VF_1477*), resulting in a partial restoration of wild-type motility. In addition, these point mutations reversed the effect of the *amiB* mutation on cellulosic biofilm production. These data are consistent with *V. fischeri* AmiB possessing amidase activity; they also suggest that AmiB suppresses cellulosic biofilm formation but promotes successful host colonization.

IMPORTANCE Peptidoglycan (PG) is a critical microbe-associated molecular pattern (MAMP) that is sloughed by cells of *V. fischeri* during symbiotic colonization of squid. Specifically, this process induces significant remodeling of a specialized symbiotic light organ within the squid mantle cavity. This phenomenon is reminiscent of the loss of ciliated epithelium in patients with whooping cough due to the production of PG monomers by *Bordetella pertussis*. Furthermore, PG processing machinery can influence susceptibility to antimicrobials. In this study, we report roles for the *V. fischeri* PG amidase AmiB, including the beneficial colonization of squid, underscoring the urgency to more deeply understand PG processing machinery and the downstream consequences of their activities.

KEYWORDS *Vibrio fischeri*, *Euprymna scolopes*, peptidoglycan, amidase, cellulose, biofilm

Vibrio fischeri is the exclusive colonist of the squid *Euprymna scolopes* (1). An array of *V. fischeri* characteristics facilitate this unique ability, such as bioluminescence,

Citation Fidopiastis PM, Mariscal V, McPherson J-M, McAnulty S, Dunn A, Stabb EV, Visick KL. 2021. *Vibrio fischeri* amidase activity is required for normal cell division, motility, and symbiotic competence. Appl Environ Microbiol 87:e02109-20. https://doi.org/10.1128/AEM.02109-20.

Editor Karyn N. Johnson, University of Queensland

Address correspondence to Pat M. Fidopiastis, pfidopia@calpoly.edu.

Received 27 August 2020
Accepted 12 October 2020
Accepted manuscript posted online 13 November 2020
Published 15 January 2021

motility, and biofilm formation (2–4). In this study, we identified an additional requirement for colonization by identifying and evaluating a biofilm-overproducing strain of *V. fischeri* carrying a transposon insertion in a gene encoding an *N*-acetylmuramoyl-L-alanine amidase (AmiB) homolog.

Amidases are Zn^{2+}-cofactored, often periplasmic enzymes that comprise one of many types of peptidoglycan (PG)-hydrolyzing enzymes in bacteria (5). Their primary activity is to cleave the amide bond between the peptide side chain and *N*-acetylmuramic acid. Thus, peptidoglycan hydrolysis by *N*-acetylmuramoyl-L-alanine amidases is a crucial step in bacterial cell division (6). Bacteria tightly regulate this process in order to encourage cytokinesis and avoid cell lysis. Cytokinesis is achieved by a collection of proteins referred to as the "divisome," which includes amidases, Z-ring-associated proteins such as FtsA, and amidase regulators (e.g., EnvC) that are believed to recruit amidases to the septum (7, 8). An additional layer of amidase regulation in *Salmonella* occurs through the activation of the two-component envelope stress response proteins CpxA and CpxR; CpxR then binds to promoters of the redundant amidases *amiA* and *amiC* to enhance expression (9). Similarly, in *Pseudomonas aeruginosa*, the cell division defects displayed by an *amiB* mutant are suppressed by the activation of the Cpx-like envelope stress response (10).

In *Escherichia coli*, four paralogous genes, *amiA*, *amiB*, *amiC*, and *amiD*, appear to act in a hierarchical manner to regulate peptidoglycan cleavage (6, 7). *P. aeruginosa* also possesses these amidase homologs but apparently requires only *amiB* and *amiC* for proper cell division (11). In support of its function in peptidoglycan cleavage, AmiB in *P. aeruginosa* possesses C-terminal LysM peptidoglycan-binding domains (10). In contrast, *Vibrio* species such as *Vibrio cholerae* and *V. anguillarum* possess a single divisome-related amidase activity encoded by *amiB* (12, 13). Rashid et al. reported that an *amiB* mutant of *V. cholerae* was defective in cell division and growth. Consistent with these pleiotropic effects, the *amiB* mutant was unable to compete with the wild type for intestinal colonization of mice. Notably, both EnvC and NlpD can promote AmiB activation in *V. cholerae*; thus, only when both activators are removed will cells of *V. cholerae* display the cell division phenotype of the *amiB* mutant (14).

The possibility that the influence of AmiB on host colonization extends beyond peptidoglycan cleavage in cell division presents an intriguing area of study. For example, there is abundant evidence that amidase activity influences biofilm formation in diverse bacteria. Núñez et al. reported an *Azotobacter* amidase mutant with defects in alginate production and suggested a link between alginate production and cell wall recycling (15). Yoshida and Kuramitsu identified a *lytR* mutant of the etiological agent of dental caries, *Streptococcus mutans*, that was deficient in biofilm production. Notably, LytR regulates genes required for amidase expression in *S. mutans* (16). Similarly, in *V. cholerae*, AmiB appears to control the switch between smooth colonies and the exopolysaccharide-producing rugose phenotype (12). Biofilm formation by cells of *V. fischeri* facilitates the colonization of squid light-organ tissue (4). In *V. fischeri*, biofilms are constructed by one of two sets of polysaccharide gene loci, *syp* and *bcs*. The importance of Syp-type biofilm in the ability of *V. fischeri* to colonize squid is established (4); however, the importance of *bcs*-encoded (cellulosic) biofilm in squid colonization is unknown. Bassis and Visick suggested that cellulosic biofilm formation might be essential in the marine environment (17). Similarly, while the regulation and role of *syp*-dependent biofilm formation are well characterized, far less is known about *bcs*. Within the *bcs* locus, *bcsA*, *bscB*, and *bcsZ* encode cellulose synthase and endoglucanase activities that are needed for cellulosic biofilm formation. Cyclic diguanylate (c-di-GMP) is required to activate the cellulose synthase, while inhibition is achieved by the cyclic diguanylate-digesting phosphodiesterase (PDE) BinA (17, 18). Phenotypically, the loss of PDE activity results in cells that overproduce cellulose and form red colonies when grown on differential medium containing Congo red dye. Taken together, cellulosic biofilm formation is greatly influenced by c-di-GMP and perhaps some as-yet-undescribed environmental conditions.

In this study, we confirm several traditional roles for AmiB in *V. fischeri* (14, 19) and

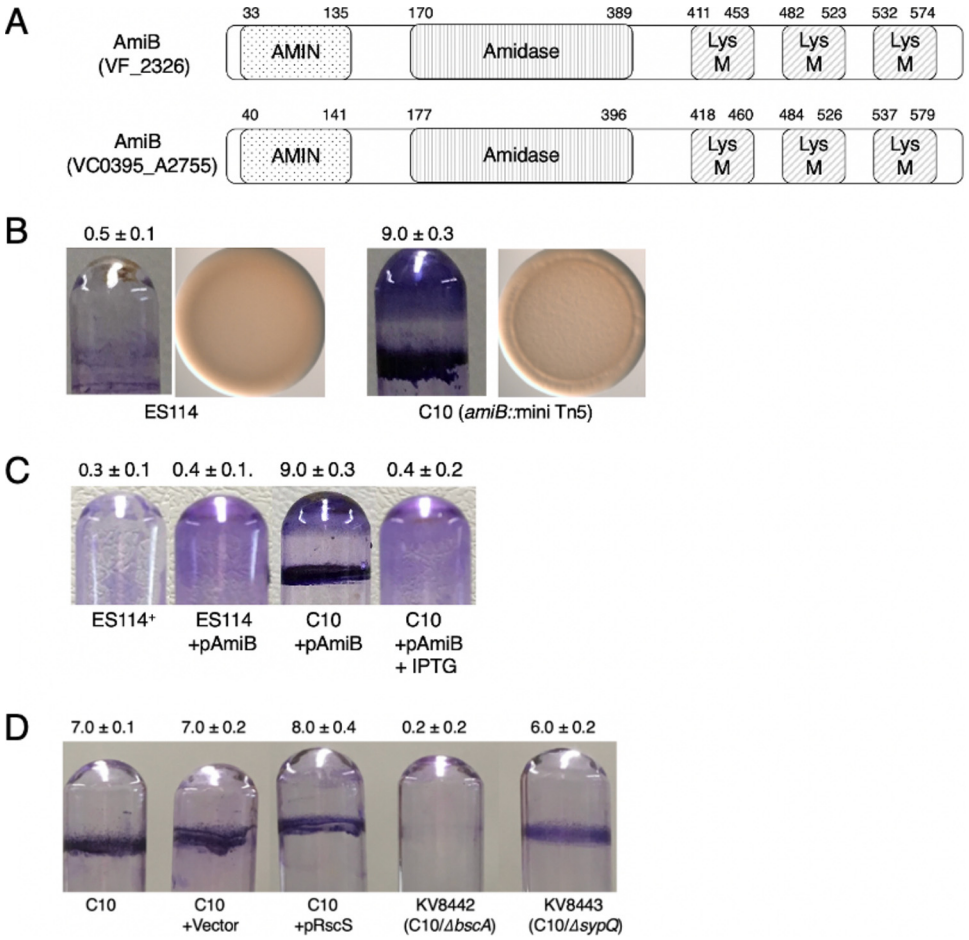

FIG 1 The amidase is a *V. cholerae* homolog that controls biofilm production. (A) *V. fischeri* AmiB shares major functional domains with the *V. cholerae* homolog. AMIN, domain. (B) Comparison of crystal violet-stained biofilms and colony architecture between the *amiB* mutant (C10) and the *V. fischeri* wild type (ES114). (C) Comparison of biofilms in wild-type and C10 strains carrying pAmiB with or without *amiB* induction by IPTG. (D) Comparison of biofilms in C10 in which the Syp biofilm regulator RscS is overexpressed on pRscS or in combination with mutations in either gene required for *syp* or *bcs* biofilm formation. Strains tested include C10, C10 carrying a vector (pKV69), C10/pRscS (pKG11), C10 Δ*bcsA* (KV8442), and C10 Δ*sypQ* (KV8443). The specific biofilm density is indicated above each tube and represents the average (± standard error) for three separate trials.

describe novel roles in cellulosic biofilm regulation and squid colonization. Furthermore, we identify and characterize suppressor mutants that arose in an *amiB* mutant population, uncovering a function for a previously unknown gene, *VF_1477*.

RESULTS

Disruption of *amiB* results in increased biofilm production. A screen of 2,000 *V. fischeri* mutants resulted in 78 with ≥2-fold increased or ≤2-fold reduced biofilm formation as indicated by crystal violet staining. Of these mutants, one of the more substantially altered was strain C10, which produced excess biofilm. Sequence analysis revealed that C10 contained an insertion in *VF_2326*. This gene encoded an amino acid sequence sharing all major functional domains and approximately 62% identity (79% similarity) across nearly the entire sequence with *V. cholerae* AmiB (Fig. 1A). Based on this homology and our evidence described below, we conclude that *VF_2326* is the *V. fischeri amiB* homolog. Quantitation of crystal violet staining of biofilms produced by C10 showed that this mutant had an ~18-fold increase in staining relative to the wild-type strain. Similarly, colonies of C10 lacked the smooth-colony phenotype of its ES114 parent but rather exhibited noticeably bumpy architecture relative to ES114 (Fig. 1B).

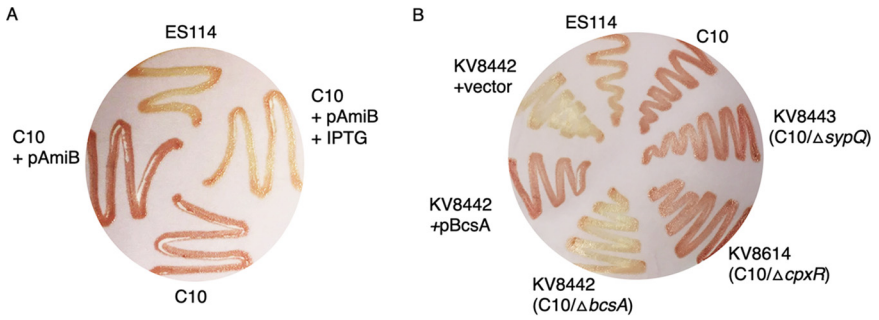

FIG 2 The *amiB* mutant overproduces cellulosic biofilm. (A) Congo red staining reveals that the biofilm formed by the *amiB* mutant is composed of cellulose. Strains tested include ES114, C10 (*amiB*::mini-Tn), and C10/pAmiB grown either with or without added IPTG to induce *amiB* expression. (B) Confirmation that increased cellulosic biofilm in the *amiB* mutant requires *bcsA* and not *sypQ* or *cpxR*. Strains tested include ES114, C10, C10 Δ*sypQ* (KV8443), C10 Δ*cpxR* (KV8614), C10 Δ*bcsA* (KV8442), and C10 Δ*bcsA* (KV8442)/pBcsA grown either with or without added IPTG to induce *bcsA* expression. Where IPTG was required (e.g., expression from pAmiB and pBcsA), IPTG was added to broth containing cells prior to streaking onto the plates. Shown are typical results from three separate trial plates.

The expression of *amiB* in strain C10 restored biofilm formation to wild-type levels (Fig. 1C), confirming that the disruption of *amiB* was responsible for the increased biofilm phenotype.

Because biofilm formation by *V. fischeri* depends on two distinct polysaccharides, symbiosis polysaccharide (SYP) and cellulose (*bcs*) (20), we next asked which one(s) was affected by *amiB* disruption (Fig. 1D). To evaluate SYP-dependent biofilm formation, we (i) overexpressed the positive regulator RscS and (ii) disrupted the structural gene *sypQ*. Neither manipulation substantially affected biofilm formation by C10. In contrast, when we disrupted *bcsA*, one of the genes for cellulose synthase, the distinctive *amiB* mutant phenotype was abolished. These data suggest that AmiB inhibits cellulose-dependent biofilm formation by *V. fischeri*.

Confirmation that excess biofilm in the *amiB* mutant depends on *bcsA*. A more typical assay for cellulose-dependent biofilm formation is Congo red binding (17, 21). Therefore, we next assessed Congo red binding by the *amiB* mutant. When strain C10 was streaked onto Congo red-containing medium (CRM), the resulting cell growth was stained a dark hue of red relative to ES114, supporting the conclusion that the biofilm of C10 is primarily composed of cellulose (Fig. 2A). Furthermore, this increased staining was complemented by expressing *amiB* in *trans* in C10, restoring the wild-type phenotype. Consistent with the crystal violet staining results, Congo red staining was not disrupted when the amidase mutation was combined with *sypQ* (Fig. 2B). Similarly, it was also not disrupted by mutation of *cpxR*, which in *Salmonella* encodes a protein that promotes the transcription of the amidase-encoding genes *amiA* and *amiC* (9). However, the deletion of *bcsA* in the *amiB* mutant background resulted in a loss of Congo red staining, supporting the conclusion that the increased biofilm phenotype of the *amiB* mutant was due to cellulose. Consistent with that conclusion, the expression of *bcsA* in *trans* restored the excess cellulosic biofilm phenotype to the *amiB-bcsA* mutant.

Disruption of *amiB* results in cells with altered morphology and arrangement. Others have reported cells of planktonic *amiB* mutants displaying an aberrant morphology (10, 14). Similarly, planktonic cells of the *V. fischeri* amidase mutant (C10) formed long chains, in contrast to the separated cells of the wild-type strain (Fig. 3A and B). Notably, cells of the wild type ranged from 1 to 2 μm in length, while chained cells of the mutant ranged from 4 to 5 μm (Fig. 3B), and the depth of the invagination is sufficient to clearly see each chained cell individually. Despite this phenotype, the growth curves of the *amiB* mutant showed no substantial defect relative to the wild-type parent (data not shown). The chaining phenomenon was also evident in biofilm-associated C10 cells (Fig. 3F to H). In addition, many of the biofilm-associated C10 cells

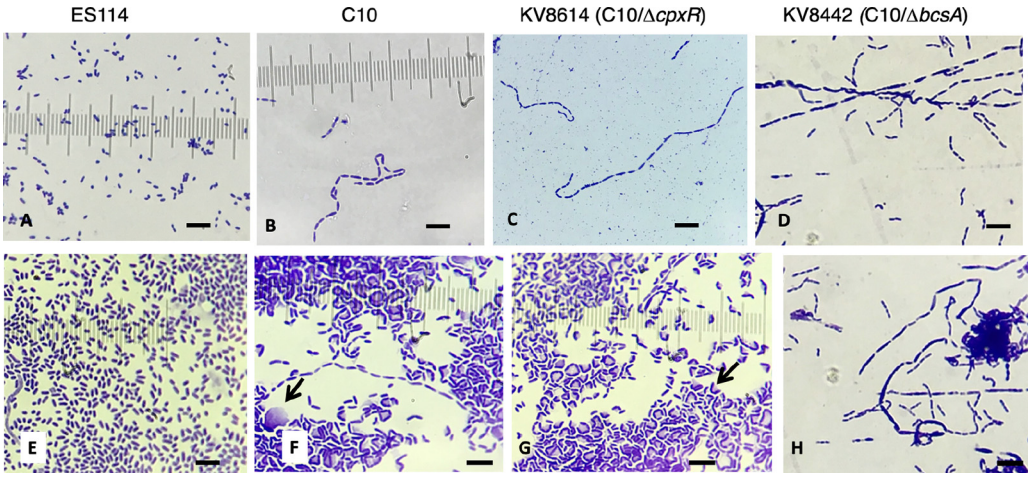

FIG 3 The *amiB* mutant is defective in cell arrangement. Comparisons of crystal violet-stained cells of planktonic (A to D) and biofilm-associated (E to H) *V. fischeri* strains are shown. Strains tested include ES114, C10, C10 Δ*cpxR* (KV8614), and C10 Δ*bcsA* (KV8442). The arrows in panels F and G point to a representative bleb. The removal of *bcsA*, but not *cpxR*, appears to eliminate blebbing (G and H). Each panel shows a typical result from 10 randomly viewed fields in three separate trials. Bars = 5 μm.

appeared to produce "blebs" of either cellular contents or secreted polysaccharide (Fig. 3F and G, arrows). Combining the *amiB* mutation with deletions in either *cpxR* or *bcsA* did not affect the cell arrangement relative to strain C10 (Fig. 3C, D, G, and H); however, blebs were not evident in combination with the *bcsA* mutation (Fig. 3D and H). These data indicate that the increased biofilm of the C10 mutant is not due to chaining *per se* but is due to some other consequence of the loss of amidase function.

Timing of AmiB activity. To determine how quickly AmiB can exert its activity, we evaluated the ability of the C10 mutant chains to be separated into individual cells following the induction of AmiB production. We found that when *amiB* expression was induced from a plasmid, the chaining phenotype of strain C10 was largely lost within 15 min (Fig. 4). These data indicate that (i) AmiB activity (and, thus, likely the *amiB* complementation plasmid) seems to be distributed throughout the length of the chained cells and (ii) despite the long length of the chained cells, with potentially physiologically distinct properties, AmiB could act quickly to separate the individual cells.

AmiB activity is regulated by two LytM-containing regulators. In *V. cholerae*, the activity of AmiB is regulated by two LytM (peptidase M23) family proteins, EnvC and NlpD (14). We thus wondered whether the same would be true for *V. fischeri*, which possesses homologs of EnvC and NlpD (VF_2351 and VF_2068) that each share ≥65% similarity and all major functional domains with their *V. cholerae* counterpart (Fig. 5A). As with *V. cholerae*, the inactivation of either of these regulators was not sufficient to abolish AmiB activity. The inactivation of both regulators, however, produced a chaining phenotype similar to that of the *amiB* mutant (Fig. 5B). Furthermore, the chaining phenotype of the *envC nlpD* double mutant could be suppressed by the overexpression of *amiB* in *trans*. Finally, the double mutant also produced colonies with a darker hue of red on Congo red medium, phenocopying the *amiB* mutant (data not shown). Together, these data suggest that the activity of AmiB is controlled by EnvC and NlpD.

Disruption of *amiB* results in a squid colonization defect. Given the cell-chaining and biofilm phenotypes of the *amiB* mutant, we asked if AmiB was important for symbiotic colonization. Notably, because turbidity measurements (i.e., optical density at 600 nm [OD_{600}]) did not correlate well with CFU per milliliter, we conducted parallel experiments in which sets of squid were exposed to a different dilution of cells. Indeed, in squid exposed to 1:1 inoculations of the amidase mutant (C10) and wild-type *V. fischeri* strain ES114, C10 was completely outcompeted by the wild type for squid colonization. In all three competition trials, 100% of isolates from squid homogenates were the wild type (Fig. 6A). However, in single-strain squid inoculation

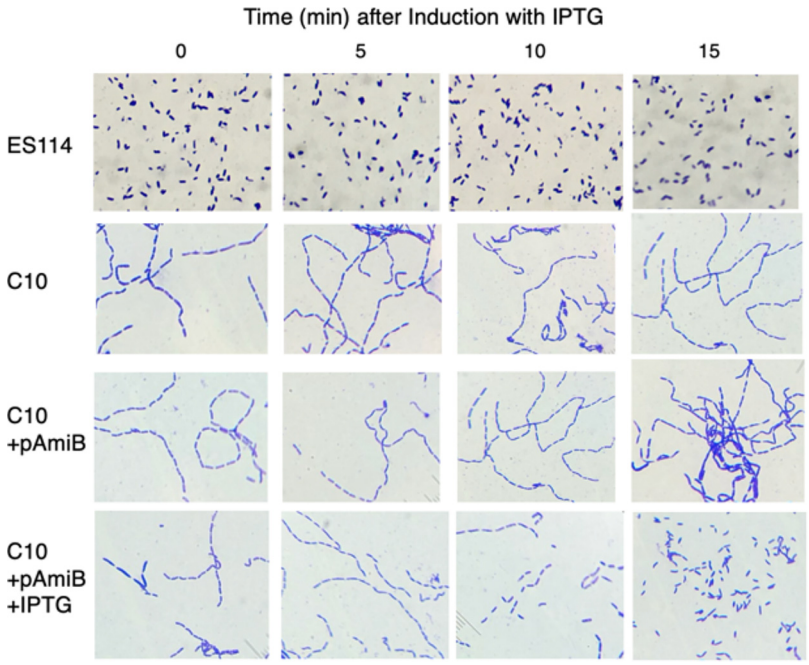

FIG 4 Kinetics of the loss-of-chaining phenotype following IPTG induction of the complemented *amiB* mutant. Each panel shows a typical result from three trials in which 10 random fields of crystal violet-stained planktonic cells were viewed at the indicated times following IPTG induction. Strains tested include ES114, C10 (*amiB*::mini-Tn), and C10/pAmiB grown either with or without added IPTG to induce *amiB* expression.

experiments, in which colonization efficiency was based on luminescence emission from squid, strain C10 gradually achieved a peak of an ~60% colonization efficiency by 48 h, whereas the wild type achieved 100% colonization by 24 h and maintained this level of colonization for at least 48 h (Fig. 6B).

Disruption of *amiB* results in loss of motility. The severe squid colonization defect led us to wonder if the *amiB* mutant has a defect in motility, as motility is a critical colonization determinant. Indeed, when the amidase mutant (C10) was spotted onto semisolid Tris-buffered seawater with $MgSO_4$ (TBS-$MgSO_4$), the cells failed to migrate from the initial spot after a 12-h incubation, while the wild-type strain migrated across the plate in about 6 h (Fig. 7A). The expression of *amiB* in *trans* alleviated this motility defect, indicating that AmiB is indeed required for *V. fischeri* motility. This result is consistent with those reported previously (19). Intriguingly, by 24 h, "flares" of motility appeared from the original C10 spot (Fig. 7B), suggesting that a mutation(s) arose that could suppress the motility defect of C10. Indeed, when we collected cells from individual flares, purified them, and retested them for motility, we found that these strains (S1 to S4) had increased motility relative to C10, although they did not have the same rate of motility as ES114 (Fig. 7C). This intermediate motility phenotype, and the fact that they retained the erythromycin resistance of their C10 parent, suggested that the *amiB* mutation was intact and that these strains had acquired an additional mutation that promoted motility.

Acquired motility in the *amiB* mutant is the result of suppressor mutations in *VF_1477*. To determine the cause of the increased motility in strains S1 to S4, we performed whole-genome sequencing. Each of these strains had a mutation in *VF_1477*, a gene of unknown function, but the presence of Sel1 repeats and a DnaJ domain (E = 1.9e−8) suggests that it might be a chaperone in the stress response (22, 23). Notably, VF_1477 is conserved in other *Vibrio* species (Table 1). Two of these mutations were expected to disrupt *VF_1477* function (S2 and S3), as they result in premature stop codons, while the consequences of the other two mutations (S1 and S4) are less clear. In mutant S1, a nonpolar valine was replaced with an acidic glutamic acid in a

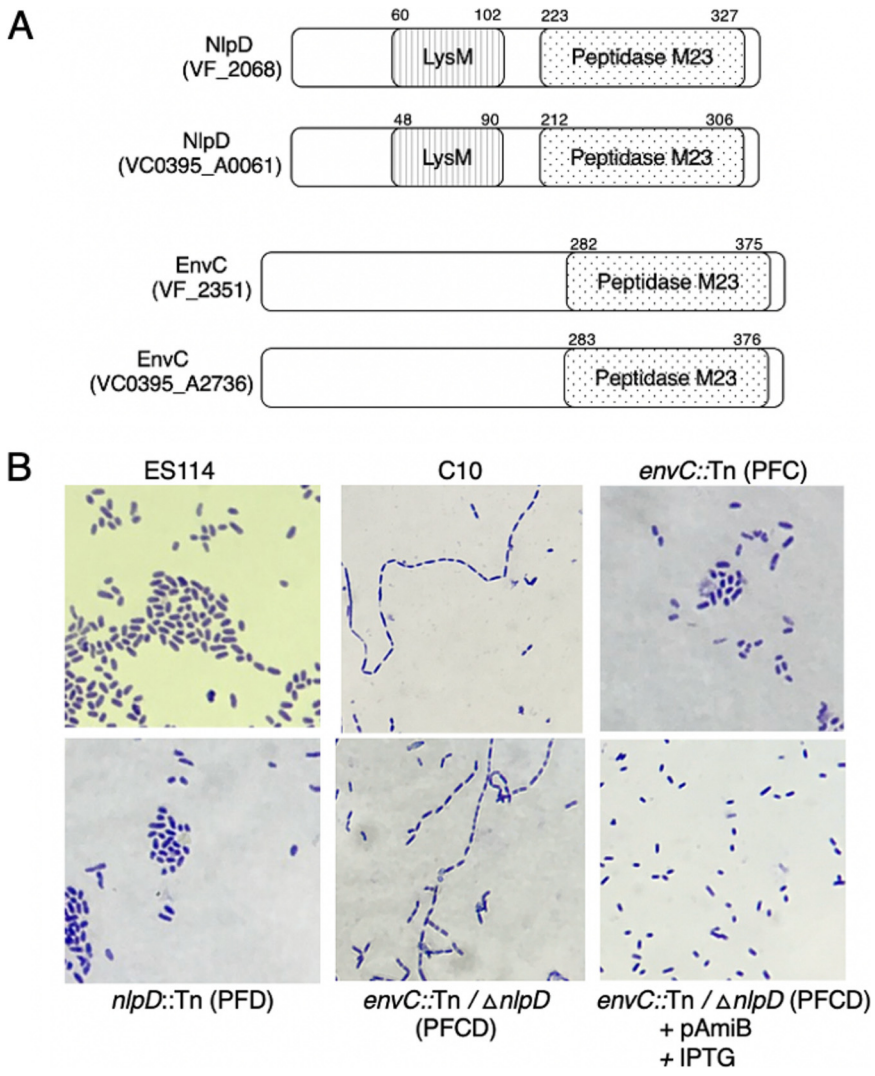

FIG 5 AmiB activity is regulated by EnvC and NlpD. (A) Both *V. fischeri* regulators (VF_2068 and VF_2351) share major functional domains with their respective *V. cholerae* homologs (VC0395_A0061 and VC0395_A2736). (B) Planktonic cells of each strain were stained with crystal violet to visualize the effects on cellular arrangement. Strains tested include ES114, C10 (*amiB*::mini-Tn), *envC*::mini-Tn*5* (PFC), *nlpD*::mini-Tn*5* (PFD), *envC*::mini-Tn*5* Δ*nlpD* (PFCD), and *envC*::mini-Tn*5* Δ*nlpD* (PFCD), induced to express *amiB* from pAmiB with IPTG. Each panel shows a typical result from 10 randomly viewed fields in three separate trials.

region of the protein with very low homology to an anti-sigma factor K domain (E value = 0.25). In mutant S4, an acidic glutamic acid replaced a nonpolar glycine in a region of the protein with high homology to a Sel1 repeat domain (E = 1.7e−10). To further understand the role of *VF_1477*, we deleted this gene in both the wild-type and *amiB* mutant backgrounds and assessed both motility and the cell-chaining phenotype (Fig. 8). Both the motility and cell arrangement of the *VF_1477* mutant were identical to those of the wild type. Consistent with the findings for the suppressor mutants, the Δ*amiB* Δ*VF_1477* double-deletion mutant exhibited partially increased motility relative to the *amiB* single mutant but did not increase motility to the level of the wild-type strain. This increase in motility could be complemented by the expression of VF_1477 in *cis*. In contrast to the results observed for motility, disruption of *VF_1477* did not alter the microscopic appearance of the cells: the single mutant phenocopied the wild-type strain, while the double mutant phenocopied the *amiB* single mutant. Finally,

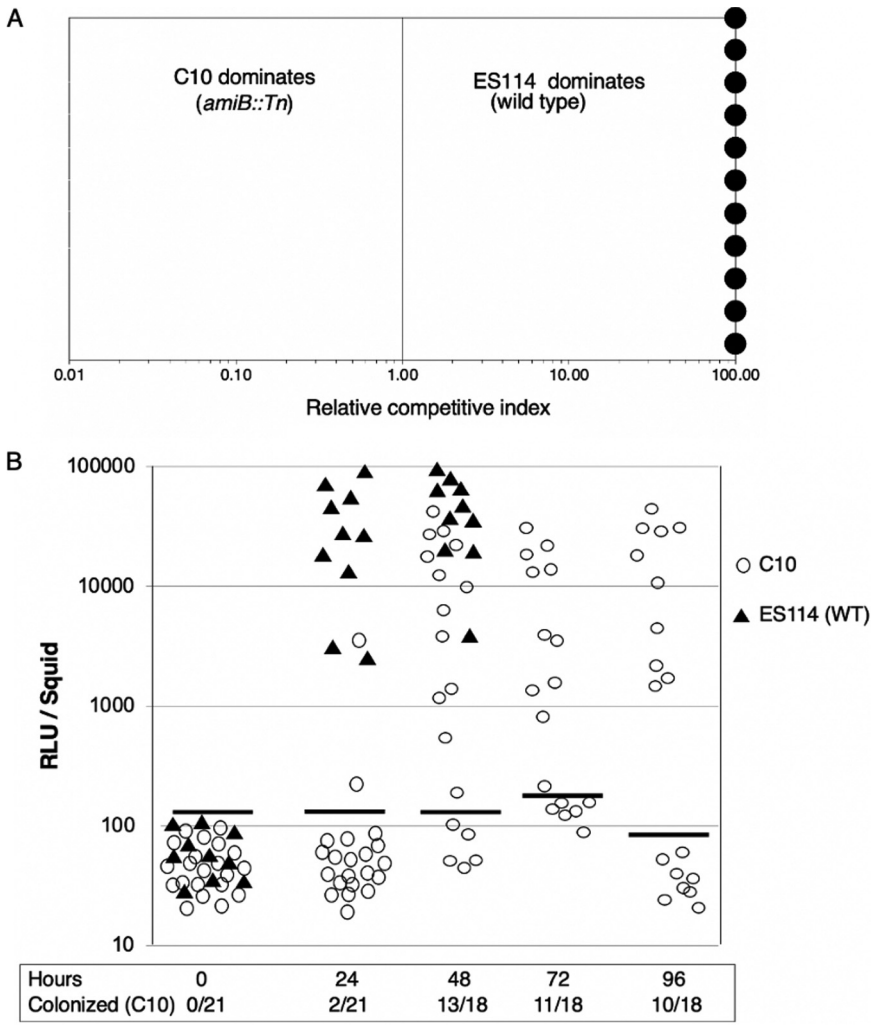

FIG 6 Squid colonization defect in the *amiB* mutant (C10). (A) Relative proportions of C10 to wild-type cells in each squid light organ 24 h after exposure to the bacteria, represented by closed black circles. (B) Kinetics of single-strain colonization of squid by strain C10. Each open circle represents bioluminescence emission by a squid colonized by strain C10 for up to 96 h. Each closed triangle represents bioluminescence emission by a squid colonized by the wild type (WT) (ES114) for up to 48 h. Black lines represent peak relative light units (RLU) of aposymbiotic squid. The number of colonized squid was determined by comparing RLU emissions between aposymbiotic squid and those exposed to strain C10. Results shown are typical for three independent trials.

neither disruption of nor complementation with *VF_1477* altered the observed "blebbing" of the *amiB* mutant.

***VF_1477* plays a role in biofilm formation.** Because motility and biofilm formation are typically inversely controlled (18, 24), and because disruption of *VF_1477* increases motility, we wondered if *VF_1477* could control biofilm formation. Indeed, the loss of *VF_1477* alone almost completely eliminated biofilm production; levels of crystal violet-stained material were ~10-fold lower than those for the wild-type parent (Fig. 9). Consistent with the findings in Fig. 1, the loss of *amiB* resulted in a significant increase in biofilm formation; this increase was also abolished by disruption of *VF_1477*, resulting in wild-type-like levels of biofilm formation. The expression of *VF_1477* in *cis* complemented the double mutant, restoring the levels of biofilm production to that of the *amiB* single mutant. These data thus provide new insight into this novel consequence of *amiB* disruption.

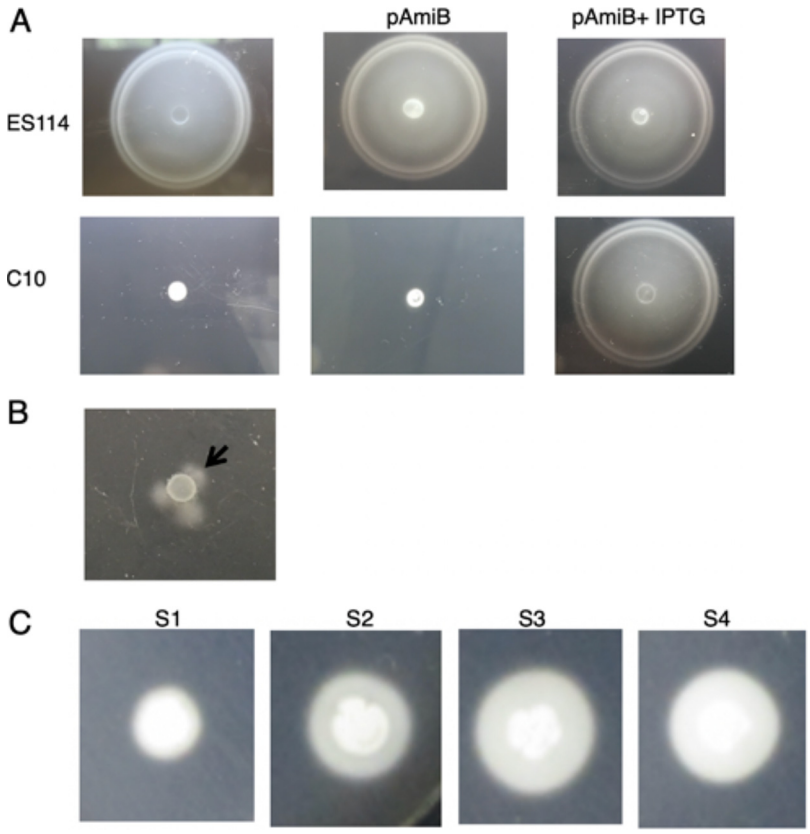

FIG 7 The *amiB* mutant is defective in motility. (A) Comparison of wild-type and *amiB* mutant (C10) motilities. The motility defect of C10 can be complemented with pAmiB but only when IPTG is added to induce the expression of *amiB*. (B) Motility "flares" (arrow) emerging 12 h after spotting strain C10 on soft agar. (C) Motility phenotypes of 4 suppressor mutants isolated from the flares (S1 to S4). Results shown are typical for three independent trials.

DISCUSSION

In this study, we investigated the pleiotropic effects of an *amiB* mutation in *V. fischeri* in order to better understand how amidases influence physiology and host colonization. Analysis of the *V. fischeri* genome revealed a single amidase gene encoding an AmiB homolog with a conserved signal peptide cleavage site, suggesting that it is

TABLE 1 Genetic characterization of *amiB* suppressor mutants S1 to S4

Strain	Mutation (gene; genotype)
ES114	Wild type
C10	*VF_2326* (*amiB*); *amiB*::mini-Tn*5*
S1	*VF_2326* (*amiB*); *amiB*::mini-Tn*5* *VF_1477*; 443T>A (Val→Glu)
S2	*VF_2326* (*amiB*); *amiB*::mini-Tn*5* *VF_1477*; 302,303delAC
S3	*VF_2326* (*amiB*); *amiB*::mini-Tn*5* *VF_1477*; 79G>T (Glu→stop)
S4	*VF_2326* (*amiB*); *amiB*::mini-Tn*5* *VF_1477*; 245G>A (Gly→Glu)

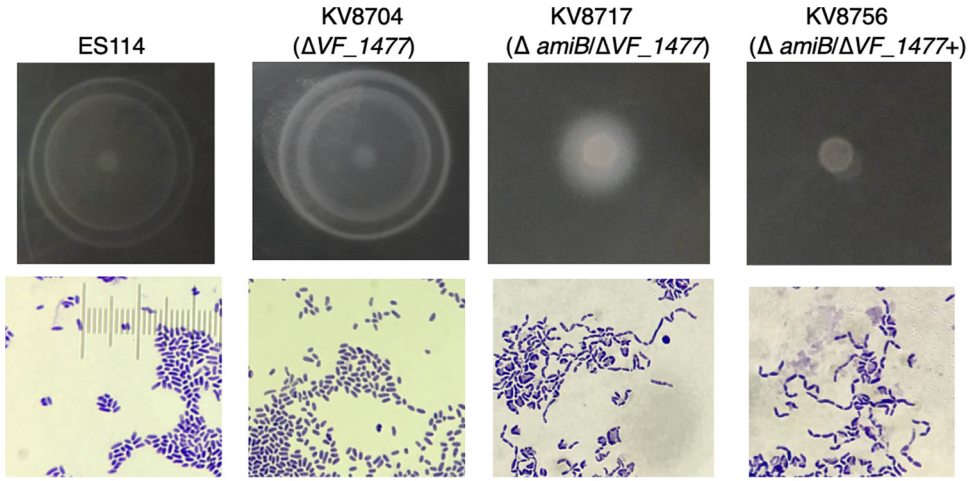

FIG 8 Effects of *amiB* and *VF_1477* on motility and cell arrangement. Disruption of *VF_1477* partially restores the defect in motility (top) but not in cell arrangement in the *amiB* mutant (bottom). These results were determined using wild-type strain ES114 and mutants Δ*VF_1477* (KV8711), Δ*amiB* Δ*VF_1477* (KV8717), and Δ*amiB* Δ*VF_1477* complemented with *VF_1477* driven by a cellobiose-inducible promoter (KV8756). The plus symbol indicates the addition of 0.1% cellobiose. Results for motility are typical for three independent trials. Each panel shows a typical result from 10 randomly viewed fields.

secreted by the Sec system like the other AmiB homologs. Consistent with this discovery, the inactivation of *amiB*, or both genes encoding its positive regulators in *V. fischeri* (e.g., *nlpD* and *envC*), was sufficient to disrupt normal cell division. Furthermore, the inactivation of *amiB* virtually abolished motility. The defective motility displayed by the *amiB* mutant is consistent with its inability to compete with the wild type for squid colonization. However, despite the motility defect, we were surprised that the mutant could still colonize squid in single-strain inoculation studies albeit with a significant delay. The delayed colonization by the *amiB* mutant was consistent with the observation of motile suppressor mutants emanating from the point of inoculation on a motility plate. Notably, whole-genome sequence analysis of several motile suppressors revealed single nucleotide variations (SNVs) in a specific gene of unknown function (*VF_1477*). Our studies also revealed that the inactivation of *amiB* resulted in a profound increase in cellulosic, but not Syp, biofilm production. Indeed, an *amiB bcsA* double mutation completely abolished biofilm production.

Shared genomic synteny among the *amiB* homologs in *V. fischeri*, *E. coli*, and *V. cholerae* (data not shown) provided preliminary evidence that they might share functions. However, there are differences between these species as to the specific types of ami-

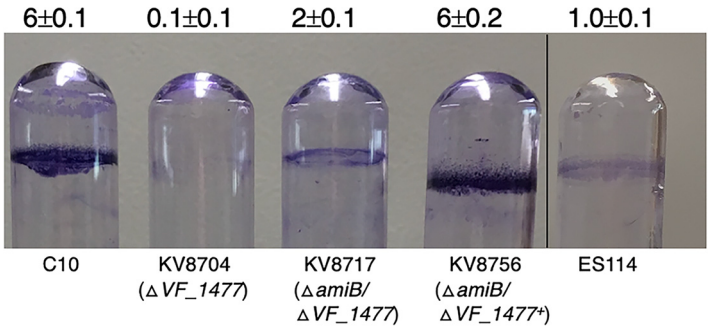

FIG 9 Effects of *amiB* and *VF_1477* disruption on biofilm formation. Biofilm formation of the following strains was assessed using the crystal violet assay: *amiB*::mini-Tn (C10), Δ*VF_1477* (KV8711), Δ*amiB* Δ*VF_1477* (KV8717), Δ*amiB* Δ*VF_1477* complemented with *VF_1477* driven by a cellobiose-inducible promoter (KV8756), and wild-type strain ES114. The plus symbol indicates the addition of 0.1% cellobiose. The specific biofilm density is indicated above each tube and represents the average (± standard error) for three replicates.

dases present and their role in the cell. For example, *E. coli* possesses three periplasmic amidases (AmiA, AmiB, and AmiC), and *P. aeruginosa* possesses two (AmiA and AmiB), while *Vibrio* species possess only one (AmiB) (10, 13, 14, 25). Not surprisingly, in *E. coli*, no single amidase is responsible for the chaining phenotype (6). In fact, the periplasmic amidases have different substrate preferences. AmiC preferentially removes tetrapeptide fragments from cross-linked peptidoglycan fragments, while AmiA and AmiB appear to prefer to cleave pentapeptides (6). Adin et al. reported that *V. fischeri* possesses homologs of *E. coli* peptidoglycan synthesis and recycling pathways, with minor differences in peptidoglycan processing homologs (26). Our study confirmed that differences exist between the peptidoglycan processing machineries of *E. coli* and *V. fischeri*. Other studies reported that the lipoprotein NlpD and the protease EnvC activate amidase activity in *E. coli* and *V. cholerae* (14, 27, 28). In *E. coli*, EnvC activates AmiA and AmiB, while NlpD activates AmiC. However, in *V. cholerae*, both EnvC and NlpD are required to activate AmiB. *V. fischeri* possesses homologs of both LytM motif-containing proteins, EnvC and NlpD, and not unexpectedly, an *envC nlpD* double mutant formed chains like the *amiB* mutant. These findings suggest a conserved function for EnvC and NlpD in AmiB regulation in these two *Vibrio* species.

Our data support and extend the findings of Brennan et al. that the loss of AmiB in *V. fischeri* results in defective cell division (i.e., chaining) (19). Yakhnina et al. pointed out subtle differences between the chaining phenotypes of *E. coli* and *P. aeruginosa*, such as the depth and positioning of cell constrictions in chained cells. *E. coli* chains seemed to possess deeper, more frequent invaginations, resulting in more clearly defined, shorter cells, while cells in chains of *P. aeruginosa* appear longer, with shallower cleavage, resulting in chains that more closely resemble filaments (10). In this study, *V. fischeri* chains appear to be more similar to those of *P. aeruginosa* in cell length but more similar to *E. coli* in the depth of invaginations. Thus, while *V. fischeri* resembles *P. aeruginosa* with respect to the major purpose of AmiB in cell division, subtle differences in the chaining phenotype suggest that different accessory proteins might be required for proper cell division.

The loss of AmiB resulted in a mutant with increased biofilm production. Bassis and Visick identified a "bacterial cellulose biosynthesis" (*bcs*) cluster in *V. fischeri* and reported its importance in cellulosic biofilm production (17). When we deleted the cellulose synthase (*bcsA*) in the *amiB* mutant, the resulting double mutant failed to produce biofilm. In addition, cells of the double mutant ceased to produce a bleb that could be excess exopolysaccharide, similar to what was reported for *Grimontia hollisae* (29). These data suggested that the loss of AmiB perturbs the regulation of the *bcs* operon, resulting in excess biofilm formation. Previous work supports a potential role for amidases in biofilm formation in a wide range of bacteria (12, 15, 16). For example, in *Azotobacter vinelandii*, the loss of the *ampDE* operon, in which *ampD* encodes a cytosolic amidase, results in increased alginate biofilm production (15). Apparently, AmpD and AmpE negatively regulate *algD*, which encodes an alginate synthase. Interestingly, the *ampDE* mutant also forms chains, like the various *amiB* mutants. In many types of bacteria, cells switch between smooth and rugose (rough) colony morphologies (29–31); in the rugose phenotype, exopolysaccharide production is turned "on." Rashid et al. screened a *V. cholerae* transposon insertion library for strains that were defective in the transition from a smooth to a rugose colony morphology (12). Those authors reported several mutants with transposon insertions in genes required for lipopolysaccharide (LPS) biosynthesis as well as genes within the *Vibrio* polysaccharide operon. Consistent with our findings, those authors also reported that an *amiB* mutant was defective in cell morphology, motility, and making the switch to a rugose phenotype. In *G. hollisae*, an abundance of elongated cells in rugose colonies led the authors to conclude that disrupted cell division enhances exopolysaccharide production (29). Taken together, these data support a model in which cell division is tightly linked to exopolysaccharide production in a diversity of microbes. In *Salmonella enterica* serovar Typhimurium, two of the Tat-secreted amidases, AmiA and AmiC, appear to be

regulated by the "envelope stress response" two-component system CpxR/CpxA (9). Similarly, in *V. cholerae*, mutation of *amiB* activated the Cpx two-component system (32). In *E. coli*, CpxR and CpxA regulate amidase activity and also appear to regulate cellulosic biofilm production (33). In this case, the activation of the envelope stress response leads to increased levels of the phosphorylated response regulator CpxR and repression of the cellulosic biofilm activator cyclic di-GMP. *V. fischeri* possesses homologs of *cpxR* and *cpxA*. Thus, we hypothesized that the loss of *amiB* and subsequent defects in cell division might somehow be connected to the envelope stress response and c-di-GMP production. However, the cellulosic biofilm phenotype of an *amiB cpxR* double mutant was indistinguishable from that of the *amiB* mutant (C10), suggesting that the biofilm phenotype of the AmiB mutant might not be due to the envelope stress response. Future work on the mechanism by which AmiB contributes to the regulation of cellulosic biofilm will hopefully shed light on the role of *bcs* genes in *V. fischeri* ecology.

We also discovered that strain C10 is severely defective in symbiotic colonization of squid. In addition to motility, several features of *V. fischeri* contribute to it being the sole colonist of *E. scolopes* light organs, such as Syp-type biofilm production and optimal levels of bioluminescence (2, 3, 34, 35). However, we did not detect a bioluminescence defect in strain C10 (data not shown). In competition experiments, the *amiB* mutant was completely outcompeted by the wild type for colonization of the squid light organ. However, when strain C10 alone was exposed to squid, the cells were able to colonize albeit after a significant delay not seen in the wild type. In *Salmonella*, repression of cellulosic biofilm promotes host colonization (36, 37). Conversely, enhanced production of cyclic di-GMP, the positive regulator of cellulosic biofilm, interferes with flagellum-based motility in *V. cholerae* and *Salmonella* (18, 36). Specifically, Zorraquino et al. reported a dual purpose for cyclic di-GMP in blocking flagellar rotation through YcgR and BcsA and cellulose production. In the latter case, cellulose fibrils physically inhibit flagellar rotation (18). These findings are consistent with the excess cellulosic biofilm and diminished motility phenotypes demonstrated by strain C10. In support, the Δ*amiB* Δ*VF_1477* double mutant displayed diminished biofilm production compared to the *amiB* single mutant and was significantly more motile. Taken together, our findings suggest that cellulose production in *V. fischeri*, like *Salmonella*, might play an indirect role in host colonization, possibly through its effect on motility. Perhaps, by defining a set of natural conditions in which cellulosic biofilm production is significantly expressed, we might eventually determine the full extent of its role in the ability of *V. fischeri* to persist in the environment and colonize squid.

We hypothesize that the temporal increase in the colonization efficiency of the *amiB* mutant might be due to the evolution of motile suppressor mutants such as those that we identified with SNVs in gene *VF_1477*. Analysis of the amino acid sequence using SignalP revealed a signal peptide cleavage site, suggesting that it most likely is secreted through the Sec system (data not shown). The presence of Sel1 domains in the encoded protein might be required for the assembly of macromolecular complexes (22). Sel1-containing proteins appear to play diverse roles in a variety of pathogens, including regulating genes within the Fur regulon of *Neisseria meningitidis* (38). In *Vibrio* species, including *V. fischeri*, the Sel1-containing protein MotX is part of its sodium-driven flagellar motor (39). In this study, the deletion of *VF_1477* in the nonmotile *amiB* mutant partially restored motility, suggesting a possible role for VF_1477 in the functioning of flagellar motor proteins. However, our current methodology is not sensitive enough to detect an obvious phenotype when VF_1477 is disrupted in otherwise wild-type cells. For now, we can conclude that the role of VF_1477 in motility is apparent only when the system is perturbed (e.g., when *amiB* is disrupted). For the future, we plan to study the colonization phenotype of the *VF_1477* mutant as well as test the hypothesis that interactions between MotX and the VF_1477 protein are important in flagellar assembly and function. Hussa et al. reported that the flagellar regulator FlrC also appears to regulate biofilm formation (40). Furthermore, Visick et al.

TABLE 2 *V. fischeri* strains constructed and/or used in this study[a]

Strain	Genotype, characteristic(s), and/or purpose	Reference
C10	*amiB*::mini-Tn*5* Erm^r; amidase mutant	This study
C10/RscS	C10$^+$/pRscS Cm^r; mutant expressing biofilm regulator RscS	This study
C10$^+$	C10/pAKD601::*amiB*; complemented AmiB mutant	This study
ES114	Wild type	2
KV7894	Δ*bcsA*; cellulose synthase mutant	20
KV8069	Δ*sypQ*::FRT-Cm^r; glycosyltransferase mutant	20
KV8233	IG (*yeiR-glmS*)::Erm^r-trunc Trim^r	41
KV8442	Δ*bcsA amiB*::mini-Tn*5*	This study
KV8443	Δ*sypQ*::FRT-Cm^r *amiB*::mini-Tn*5*	This study
KV8578	Δ*cpxR*::FRT-Trim^r; envelope stress response regulator mutant	This study
KV8614	*amiB*::mini-Tn*5* Erm^r Δ*cpxR*::FRT-Trim^r	This study
KV8692	Δ*amiB*::FRT-Trim^r	This study
KV8693	Δ*VF_1477*::FRT-Erm^r; putative tetratricopeptide repeat protein mutant	This study
KV8711	Δ*VF_1477*::FRT	This study
KV8717	Δ*amiB*::FRT-Trim Δ*VF_1477*::FRT-Erm^r	This study
KV8756	Δ*amiB*::FRT Δ*VF_1477*::FRT IG (*yeiR-glmS*)::P*cel VF_1477*; *amiB VF_1477* double mutant complemented with *VF_1477* driven by a cellobiose-inducible promoter	This study
KV8737	Δ*amiB*::FRT Δ*VF_1477*::FRT	This study
PFC	*envC*::mini-Tn*5* Erm^r; amidase regulator mutant	This study
PFD	*nlpD*::mini-Tn*5* Erm^r; amidase regulator mutant	This study
PFCD	*envC*::mini-Tn*5* Erm^r *nlpD*::FRT	This study
PFCD/pAmiB	*envC*::mini-Tn*5* Erm^r Δ*nlpD*::FRT/pAmiB; *amiB*-complemented *envC nlpD* double mutant	This study

[a]IG, intergenic region between the genes in parentheses.

revealed that FlrA, FliQ, and possibly flagella in general interfere with cellulosic biofilm formation in *V. fischeri* (41).

Our study highlights the pleiotropic effects of amidase activity on motility, cellulosic biofilm formation, and symbiotic colonization of squid by cells of *V. fischeri*. The purpose of cell division proteins in host colonization and as targets for antimicrobials is a burgeoning area of study. Furthermore, the ways in which *V. fischeri* cells use cellulosic biofilm are not known, but the findings presented here connecting cellulose production, proper cell division, and motility provide new perspectives to study this potentially important aspect of *V. fischeri* biology.

MATERIALS AND METHODS

Strains and media. Strains, plasmids, and primers used in this study are listed in Tables 2, 3, and 4, respectively. The parent *V. fischeri* strain used in this study (e.g., ES114) was isolated from *E. scolopes* (2). Mutants of this strain were constructed either by triparental mating using *E. coli* strain CC118 *λpir* carrying helper plasmid pEVS104 (42) or by TfoX-mediated transformation (43). Gene alterations resulted from either allelic replacement or transposon insertion as described previously (41, 44). For the resolution of the FLP recombination target (FRT)-flanked antibiotic resistance cassettes, flippase plasmid pKV496 was used (41). Mutants containing the Tn*5* insertion were verified by sequencing DNA that flanked the insertion (44). For the complementation of either *amiB* or *bcsA*, the gene (including the ribosome-binding site through the stop codon) was amplified and inserted into separate pAKD601B plasmids (45). The expression of *amiB* in pAKD601B was controlled by the addition of 100 μM isopropyl-β-D-thiogalactopyranoside (IPTG), which we determined to be an optimal dose for gene expression (data not shown). For genetic manipulations, cells of *V. fischeri* were grown on LB-salt (LBS) medium as described previously (46). The liquid medium for biofilm assays (biofilm minimal medium [BMM]) was a modified HEPES minimal medium that contained artificial seawater, 0.1% (wt/vol) ammonium chloride, 0.0058% K_2HPO_4, 10 μM ferrous ammonium sulfate, 100 mM HEPES (pH 7.5), and 0.03% Casamino Acids. Biofilm production was also visualized on solid LBS agar supplemented with 40 μg/ml Congo red and 15 μg/ml Coomassie blue (LBS-CR). For squid colonization assays, *V. fischeri* cells were grown in seawater tryptone (SWT) medium (2) prior to inoculation into seawater containing squid. Where necessary, the following antibiotics were added to the growth medium: kanamycin (100 μg/ml), erythromycin (2.5 μg/ml), chloramphenicol (5 μg/ml), tetracycline (15 μg/ml), and trimethoprim (10 μg/ml). All incubations were carried out at 24°C to 28°C.

Transposon mutagenesis of *V. fischeri*. A transposon mutant library of *V. fischeri* was constructed as described previously (44). Two thousand mutants were streak purified and screened for alterations in biofilm formation using the crystal violet assay (see below). Mutants with at least a 2-fold variation in biofilm production (over- or underproduction) relative to wild-type strain ES114 were sequenced to localize the transposon insertion.

TABLE 3 Plasmids constructed and/or used in this study[a]

Plasmid	Characteristic(s)	Reference
pAKD601B	*lacI*^{q}; IPTG-inducible promoter; Kn^r	45
pAmiB	pAKD601B containing the coding sequence of *VF_2326* (*amiB*)	This study
pBcsA	pAKD601B containing the coding sequence of *bcsA*	This study
pEVS170	Mini-Tn*5* delivery plasmid	48
plostfoX	TfoX overexpression; Cm^r	43
plostfoX-Kan	TfoX overexpression; Kn^r	49
pRscS (pKG11)	RscS overexpression; Tet^r	4
pKV69	Vector for pRscS; Tet^r	50
pKV494	pJET + FRT-Erm^r	41
pKV496	pJET + flippase gene	41
pKV503	pJET + *glmS* sequences	41
pKV518	pJET + trunc Erm^r; P*cel*	41
pMLC2	pJET + FRT-Trim^r	41

[a]Erm^r, erythromycin resistance; Cm^r, chloramphenicol resistance; Trim^r, trimethoprim resistance; Kn^r, kanamycin resistance.

Determining the site of Tn*5* insertion in *V. fischeri* strains. Genomic DNA was extracted from biofilm mutants, cut with Sau3AI, and self-ligated to form closed circular DNA fragments. Next, fragments were subjected to inverse PCR using primers VIPCR-F (5′-CCTAGAGCGGCCGCAGA-3′) and VIPCR-RBio (biotin-5′-ACTGGCCGTCGTTTTACAG-3′) to amplify DNA flanking the transposon insertion. The resulting PCR amplicons were sequenced using primer MoSeq-F (5′-AGATGTGTATAAGAGAC-3′) and a pyrosequencer to identify the flanking DNA.

Biofilm assays. (i) Crystal violet. *V. fischeri* cells were grown in BMM at 28°C with shaking overnight. Biofilms formed in tubes or on glass slides were then stained with crystal violet. The cell density (OD_{600}) of each culture was determined, and the tubes were thoroughly rinsed with sterile water to remove nonadhering cells and then filled with 1% crystal violet for 5 min to stain biofilms. For the qualitative

TABLE 4 Primers used in this study

Primer	Sequence[a]	Purpose[b]
cL1	CCATACTTAGTGCGGCCGCCTA	Amplify antibiotic resistance marker
cL2	CCATGGCCTTCTAGGCCTATCC	Amplify antibiotic resistance marker
Δ*cpxR*-up-F	TCCTGCATAGCTTGGTGATC	Delete *cpxR*
Δ*cpxR*-up-R	taggcggccgcactaagtatggCAGAGCTGTCAGTTCAATATC	Delete *cpxR*
Δ*cpxR*-down-F	ggataggcctagaaggccatggTTTGTAGAGGAGTAATCGGTG	Delete *cpxR*
Δ*cpxR*-down-R	TAACGAGCATGGTAACTAAGAG	Delete *cpxR*
Δ*amiB*-Up-F	GAAATTAGTGAATAATGGAACGC	Delete *amiB*
Δ*amiB*-Up-R	taggcggccgcactaagtatggAAGAACAACAAATAGCGTATACC	Delete *amiB*
Δ*amiB*-Down-F	GGATAGGCCTAGAAGGCCATGGATTCCAACCAGTTAAGGAACAAGG	Delete *amiB*
Δ*amiB*-down-R	CCAATCGACTTAATGCAATACGC	Delete *amiB*
Δ*nlpD*-Up-F	CGAAGTATGGTTAATCGCTATT	Delete *nlpD*
Δ*nlpD*-Up-R	taggcggccgcactaagtatggATTTGCTTTGTTGCCGATATC	Delete *nlpD*
Δ*nlpD*-Down-F	ggataggcctagaaggccatggGTTTTGGCTTAGCAACCGGTT	Delete *nlpD*
Δ*nlpD*-Down-R	CTCTAGTACGAGCAGTGTACG	Delete *nlpD*
Δ*VF_1477*-Up-F	ATTGGCATCGTGATTCCGTG	Delete *VF_1477*
Δ*VF_1477*-Up-R	taggcggccgcactaagtatggAACAGCAAGTAAAACAGAACGGATC	Delete *VF_1477*
Δ*VF_1477*-Down-F	ggataggcctagaaggccatggCGATAACGTACACGGAATACGAG	Delete *VF_1477*
Δ*VF_1477*-Down-R	GCTCCAATTGCAATTGGTCTG	Delete *VF_1477*
amiBF	CTTGAGTTTATGGGGATCCGTGA	Complement *amiB* and *envC nlpD*
amiBR	GATCCCCGATCCATTATCACGGA	Complement *amiB* and *envC nlpD*
bcsAF	TGAGTTAGATAAGCAGTGC	Complement *bcsA*
bcsAR	CATTGTCACTATGAGCTGT	Complement *bcsA*
Ins-Up-F*	AAGAAACCGATACCGTTTACG	Complement *VF_1477*
c-VF1477-F	ggataggcctagaaggccatggaggaggtTTATATTTATGATCCGTTCTGTTTTACTTG	Complement *VF_1477*
c-VF1477-R	taggcggccgcactaagtatggaCTCGTATTCCGTGTACGTTATCG	Complement *VF_1477*
Ins-Down-F	TCCATACTTAGTGCGGCCGCCTA	Complement *VF_1477*
Ins-Down-R	GGTCGTGGGGAGTTTTATCC	Complement *VF_1477*
VIPCR-F	CCTAGAGCGGCCGCAGA	iPCR
VIPCR-RBio	Biotin-ACTGGCCGTCGTTTTACAG	iPCR
MoSeq-F	AGATGTGTATAAGAGAC	Tn localization

[a]All sequences are shown in the 5′-to-3′ direction. Lowercase letters indicate "tails" that are not homologous to the target being amplified.
[b]Tn, transposon.

determination of biofilm density, nonadherent crystal violet was rinsed with water, and biofilms were photographed. For the quantitative determination of biofilm density, biofilm-associated crystal violet was eluted with 95% ethanol. The OD_{600} of the eluate was then measured with a spectrophotometer. The specific biofilm density was determined by dividing the OD_{600} of the biofilm eluate by the OD_{600} of the planktonic cell density.

(ii) Colony architecture. We also used colony appearance as an indirect measure of biofilm formation. *V. fischeri* strains were grown overnight at 28°C in LBS medium. The cultures grown overnight were subcultured, grown until mid-log phase, and diluted to an OD_{600} of 0.2. Aliquots were spotted onto LBS agar and incubated for 24 h at 24°C, and the resulting growth (referred to as a "colony" for simplicity) was imaged with a Zeiss Stemi 2000-C dissecting microscope.

(iii) Congo red. Cellulosic biofilm production was visualized by streaking cells on LBS-CR plates. After incubation, streaks were overlaid with white paper to transfer the cells for easier visualization of red dye accumulation indicative of cellulose production, as described previously (20). When needed, broth cultures were supplemented with IPTG prior to streaking onto Congo red plates.

(iv) Determining cell arrangement and morphology. Planktonic cells of *V. fischeri* grown with shaking overnight in LBS broth at 28°C were aseptically smeared onto glass slides with a loop, air dried, heat fixed, and then stained with crystal violet for 1 min. Excess crystal violet was then rinsed off, and cells were visualized by bright-field microscopy. To visualize biofilm-associated cells, *V. fischeri* cells were grown in BMM at 28°C with gentle shaking overnight in 50-ml conical tubes containing a sterilized glass slide. Slides were removed from the tubes, rinsed to remove nonadhering cells, and then flooded with 1% crystal violet for 5 min. Nonadherent crystal violet was removed with sterile water, and stained biofilms were visualized by bright-field microscopy.

(v) Loss-of-chaining kinetics in the mutant due to complementation. One flask each of the wild type and mutant and two flasks of the mutant complemented with pAKD601::*amiB* were grown in LBS medium with shaking. When the flasks reached an OD_{600} of ~1.0, an aliquot of IPTG was added to one of the flasks of the complemented mutant. Subsequently, an aliquot was removed from each flask to determine cell arrangement and morphology as described above; this was repeated every 5 min for 1 h.

(vi) Motility assay. Cells of *V. fischeri* were grown at 28°C with shaking in LBS medium to mid-log phase (OD_{600} = ~0.3 to 0.4). A 10-μl aliquot of cells was spotted onto TBS-$MgSO_4$ soft agar and monitored for migration from the spot over the course of 6 h as described previously (47).

(vii) Whole-genome sequencing to characterize suppressor mutants. Genomic DNA was fragmented by sonication in iced deionized H_2O six times for 15 s at 5 W using an F60 Sonic Dismembrator (Fisher Scientific) to produce ~200-bp fragments for Illumina library construction. Genomic DNA adaptors were diluted to 15 mM prior to ligation. Sequencing was performed using an Illumina NextSeq genome analyzer at the University of Georgia Facility. Assembled reads were compared to the resequenced and published ES114 genomes as references using Geneious software.

(viii) Squid colonization assays. The symbiotic competence of mutant *V. fischeri* strains was determined either singly or in competition with the wild type. For single-strain inoculations, cells were grown to mid-log phase in SWT medium and then inoculated into separate bowls of seawater containing squid to achieve ~3,000 CFU/ml. After 3 h, squid were moved to *V. fischeri*-free seawater and monitored for luminescence over several days. For competition experiments, squid were exposed to an ~1:1 ratio of mutant to wild-type cells for 3 h. Squid were moved into *V. fischeri*-free seawater and then homogenized after 24 h to determine the ratio of wild-type to mutant cells in each light organ. The relative competitive index (RCI) was determined by dividing the wild-type-to-mutant ratio for each squid by the ratio for the inoculum. Log-transformed data were used to calculate the average RCI and determine statistical significance.

Data availability. The raw sequencing reads are available via the Sequence Read Archive (BioProject no. PRJNA674884).

ACKNOWLEDGMENTS

We thank Zomary Flores-Cruz and Spencer Nyholm (University of Connecticut, Storrs) for assisting with squid experiments. We also thank Chris Corcoran for assistance with bacterial growth curves and Macy Coppinger for assistance with whole-genome sequencing.

Undergraduate researchers V.M. and J.-M.M. were generously funded by The William and Linda Frost Fund. This work was partially supported by NSF grants IOS-0843317 awarded to P.M.F. and IOS-1557964 to E.V.S. and NIGMS grants R01 GM114288 and R35 GM130355 awarded to K.L.V.

REFERENCES

1. McFall-Ngai MJ, Ruby EG. 1991. Symbiont recognition and subsequent morphogenesis as early events in an animal-bacterial mutualism. Science 254:1491–1494. https://doi.org/10.1126/science.1962208.
2. Boettcher KJ, Ruby EG. 1990. Depressed light emission by symbiotic *Vibrio fischeri* of the sepiolid squid *Euprymna scolopes*. J Bacteriol 172:3701–3706. https://doi.org/10.1128/jb.172.7.3701-3706.1990.
3. Graf J, Dunlap PV, Ruby EG. 1994. Effect of transposon-induced motility mutations on colonization of the host light organ by *Vibrio fischeri*. J Bacteriol 176:6986–6991. https://doi.org/10.1128/jb.176.22.6986-6991.1994.
4. Yip ES, Geszvain K, DeLoney-Marino CR, Visick KL. 2006. The symbiosis regulator RscS controls the *syp* gene locus, biofilm formation and

symbiotic aggregation by *Vibrio fischeri*. Mol Microbiol 62:1586–1600. https://doi.org/10.1111/j.1365-2958.2006.05475.x.
5. Klockner A, Otten C, Derouaux A, Vollmer W, Buhl H, De Benedetti S, Munch D, Josten M, Molleken K, Sahl H-G, Henrichfreise B. 2014. AmiA is a penicillin target enzyme with dual activity in the intracellular pathogen *Chlamydia pneumoniae*. Nat Commun 5:4201. https://doi.org/10.1038/ncomms5201.
6. Priyadarshini R, de Pedro M, Young KD. 2007. Role of peptidoglycan amidases in the development and morphology of the division septum in *Escherichia coli*. J Bacteriol 189:5334–5347. https://doi.org/10.1128/JB.00415-07.
7. van Heijenoort J. 2011. Peptidoglycan hydrolases of *Escherichia coli*. Microbiol Mol Biol Rev 75:636–663. https://doi.org/10.1128/MMBR.00022-11.
8. Vollmer W, Bertsche U. 2008. Murein (peptidoglycan) structure, architecture and biosynthesis in *Escherichia coli*. Biochim Biophys Acta 1778:1714–1734. https://doi.org/10.1016/j.bbamem.2007.06.007.
9. Weatherspoon-Griffin N, Zhao G, Kong W, Kong Y, Morigen, Andrews-Polymenis H, McClelland M, Shi Y. 2011. The CpxR/CpxA two-component system up-regulates two Tat-dependent peptidoglycan amidases to confer bacterial resistance to antimicrobial peptide. J Biol Chem 286:5529–5539. https://doi.org/10.1074/jbc.M110.200352.
10. Yakhnina AA, McManus HR, Bernhardt TG. 2015. The cell wall amidase AmiB is essential for *Pseudomonas aeruginosa* cell division, drug resistance, and viability. Mol Microbiol 97:957–973. https://doi.org/10.1111/mmi.13077.
11. Al-Saigh S. 2012. MA thesis. McMaster University, Hamilton, Ontario, Canada.
12. Rashid MH, Rajanna C, Ali A, Karaolis DKR. 2003. Identification of genes involved in the switch between the smooth and rugose phenotypes of *Vibrio cholerae*. FEMS Microbiol Lett 227:113–119. https://doi.org/10.1016/S0378-1097(03)00657-8.
13. Ahn S-H, Kim D-G, Jeong S-H, Hong G-E, Kong I-S. 2006. Isolation of *N*-acetylmuramoyl-L-alanine amidase gene (*amiB*) from *Vibrio anguillarum* and the effect of *amiB* gene deletion on stress responses. J Microbiol Biotechnol 16:1416–1421.
14. Möll A, Dörr T, Alvarez L, Chao MC, Davis BM, Cava F, Waldor MK. 2014. Cell separation in *Vibrio cholerae* is mediated by a single amidase whose action is modulated by two nonredundant activators. J Bacteriol 196:3937–3948. https://doi.org/10.1128/JB.02094-14.
15. Núñez C, Moreno S, Cárdenas L, Soberón-Chávez G, Espín G. 2000. Inactivation of the *ampDE* operon increases transcription of *algD* and affects morphology and encystment of *Azotobacter vinelandii*. J Bacteriol 182:4829–4835. https://doi.org/10.1128/jb.182.17.4829-4835.2000.
16. Yoshida A, Kuramitsu HK. 2002. Multiple *Streptococcus mutans* genes are involved in biofilm formation. Appl Environ Microbiol 68:6283–6291. https://doi.org/10.1128/aem.68.12.6283-6291.2002.
17. Bassis CM, Visick KL. 2010. The cyclic-di-GMP phosphodiesterase BinA negatively regulates cellulose-containing biofilms in *Vibrio fischeri*. J Bacteriol 192:1269–1278. https://doi.org/10.1128/JB.01048-09.
18. Zorraquino V, García B, Latasa C, Echeverz M, Toledo-Arana A, Valle J, Lasa I, Solano C. 2013. Coordinated cyclic-di-GMP repression of *Salmonella* motility through YcgR and cellulose. J Bacteriol 195:417–428. https://doi.org/10.1128/JB.01789-12.
19. Brennan CA, Mandel MJ, Gyllborg MC, Thomasgard KA, Ruby EG. 2013. Genetic determinants of swimming motility in the squid light-organ symbiont *Vibrio fischeri*. Microbiologyopen 2:576–594. https://doi.org/10.1002/mbo3.96.
20. Tischler AH, Lie L, Thompson CM, Visick KL. 2018. Discovery of calcium as a biofilm-promoting signal for *Vibrio fischeri* reveals new phenotypes and underlying regulatory complexity. J Bacteriol 200:e00016-18. https://doi.org/10.1128/JB.00016-18.
21. Teather RM, Wood PJ. 1982. Use of Congo red-polysaccharide interactions in enumeration and characterization of cellulolytic bacteria from the bovine rumen. Appl Environ Microbiol 43:777–780. https://doi.org/10.1128/AEM.43.4.777-780.1982.
22. Mittl PR, Schneider-Brachert W. 2007. Sel1-like repeat proteins in signal transduction. Cell Signal 19:20–31. https://doi.org/10.1016/j.cellsig.2006.05.034.
23. Susin MF, Baldini RL, Gueiros-Filho F, Gomes SL. 2006. GroES/GroEL and DnaK/DnaJ have distinct roles in stress responses and during cell cycle progression in *Caulobacter crescentus*. J Bacteriol 188:8044–8053. https://doi.org/10.1128/JB.00824-06.
24. Watnick PI, Lauriano CM, Klose KE, Croal L, Kolter R. 2001. The absence of a flagellum leads to altered colony morphology, biofilm development and virulence in *Vibrio cholerae* O139. Mol Microbiol 39:223–235. https://doi.org/10.1046/j.1365-2958.2001.02195.x.
25. Priyadarshini R, Popham DL, Young KD. 2006. Daughter cell separation by penicillin-binding proteins and peptidoglycan amidases in *Escherichia coli*. J Bacteriol 188:5345–5355. https://doi.org/10.1128/JB.00476-06.
26. Adin DM, Engle JT, Goldman WE, McFall-Ngai MJ, Stabb EV. 2009. Mutations in *ampG* and lytic transglycosylase genes affect the net release of peptidoglycan monomers from *Vibrio fischeri*. J Bacteriol 191:2012–2022. https://doi.org/10.1128/JB.01547-08.
27. Uehara T, Parzych KR, Dinh T, Bernhardt TG. 2010. Daughter cell separation is controlled by cytokinetic ring-activated cell wall hydrolysis. EMBO J 29:1412–1422. https://doi.org/10.1038/emboj.2010.36.
28. Yang DC, Peters NT, Parzych KR, Uehara T, Markovski M, Bernhardt TG. 2011. An ATP-binding cassette transporter-like complex governs cell-wall hydrolysis at the bacterial cytokinetic ring. Proc Natl Acad Sci U S A 108:18209–18210. https://doi.org/10.1073/pnas.1107780108.
29. Curtis SK, Kothary MH, Blodgett RJ, Raybourne RB, Ziobro GC, Tall BD. 2007. Rugosity in *Grimontia hollisae*. Appl Environ Microbiol 73:1215–1224. https://doi.org/10.1128/AEM.02553-06.
30. Jobling MG, Holmes RK. 1997. Characterization of *hapR*, a positive regulator of the *Vibrio cholerae* HA/protease gene *hap*, and its identification as a functional homologue of the *Vibrio harveyi luxR* gene. Mol Microbiol 26:1023–1034. https://doi.org/10.1046/j.1365-2958.1997.6402011.x.
31. Starkey M, Hickman JH, Ma L, Zhang N, De Long S, Hinz A, Palacios S, Manoil C, Kirisits MJ, Starner TD, Wozniak DJ, Harwood CS, Parsek MR. 2009. *Pseudomonas aeruginosa* rugose small-colony variants have adaptations that likely promote persistence in the cystic fibrosis lung. J Bacteriol 191:3492–3503. https://doi.org/10.1128/JB.00119-09.
32. Slamti L, Waldor MK. 2009. Genetic analysis of activation of the *Vibrio cholerae* Cpx pathway. J Bacteriol 191:5044–5056. https://doi.org/10.1128/JB.00406-09.
33. Ma Q, Wood TK. 2009. OmpA influences *Escherichia coli* biofilm formation by repressing cellulose production through the CpxRA two-component system. Environ Microbiol 11:2735–2746. https://doi.org/10.1111/j.1462-2920.2009.02000.x.
34. Visick KL, Foster J, Doino J, McFall-Ngai M, Ruby EG. 2000. *Vibrio fischeri lux* genes play an important role in colonization and development of the host light organ. J Bacteriol 182:4578–4586. https://doi.org/10.1128/jb.182.16.4578-4586.2000.
35. Shibata S, Yip ES, Quirke KP, Ondrey JM, Visick KL. 2012. Roles of the structural symbiosis polysaccharide (*syp*) genes in host colonization, biofilm formation, and polysaccharide biosynthesis in *Vibrio fischeri*. J Bacteriol 194:6736–6747. https://doi.org/10.1128/JB.00707-12.
36. Ahmad I, Rouf SF, Sun L, Cimdins A, Shafeeq S, Guyon SL, Schottkowski M, Rhen M, Römling U. 2016. BcsZ inhibits biofilm phenotypes and promotes virulence by blocking cellulose production in *Salmonella enterica* serovar Typhimurium. Microb Cell Fact 15:177. https://doi.org/10.1186/s12934-016-0576-6.
37. Pontes MH, Lee E-J, Choi J, Groisman EA. 2015. *Salmonella* promotes virulence by repressing cellulose production. Proc Natl Acad Sci U S A 112:5183–5188. https://doi.org/10.1073/pnas.1500989112.
38. Li M-S, Langford PR, Kroll JS. 2017. Inactivation of NMB0419, encoding a Sel1-like repeat (SLR) protein, in *Neisseria meningitidis* is associated with differential expression of genes belonging to the Fur regulon and reduced intraepithelial replication. Infect Immun 85:e00574-16. https://doi.org/10.1128/IAI.00574-16.
39. McCarter LL. 1994. MotX, the channel component of the sodium-type flagellar motor. J Bacteriol 176:5988–5998. https://doi.org/10.1128/jb.176.19.5988-5998.1994.
40. Hussa EA, Darnell CL, Visick KL. 2008. RscS functions upstream of SypG to control the *syp* locus and biofilm formation in *Vibrio fischeri*. J Bacteriol 190:4576–4583. https://doi.org/10.1128/JB.00130-08.
41. Visick KL, Hodge-Hansen KM, Tischler AH, Bennett AK, Mastrodomenico V. 2018. Tools for rapid genetic engineering of *Vibrio fischeri*. Appl Environ Microbiol 84:e00850-18. https://doi.org/10.1128/AEM.00850-18.
42. Stabb EV, Ruby EG. 2002. RP4-based plasmids for conjugation between *Escherichia coli* and members of the Vibrionaceae. Methods Enzymol 358:413–426. https://doi.org/10.1016/s0076-6879(02)58106-4.
43. Pollack-Berti A, Wollenberg MS, Ruby EG. 2010. Natural transformation of *Vibrio fischeri* requires *tfoX* and *tfoY*. Environ Microbiol 12:2302–2311. https://doi.org/10.1111/j.1462-2920.2010.02250.x.
44. Stoudenmire JL, Black M, Fidopiastis PM, Stabb EV. 2019. Mutagenesis of *Vibrio fischeri* and other marine bacteria using hyperactive mini-Tn5

derivatives. *In* Ricke S, Park S, Davis M (ed), Microbial transposon mutagenesis. Methods in molecular biology, vol 2016. Humana Press, New York, NY.
45. Dunn AK, Stabb EV. 2008. Genetic analysis of trimethylamine *N*-oxide reductases in the light-organ symbiont *Vibrio fischeri* ES114. J Bacteriol 190:5814–5823. https://doi.org/10.1128/JB.00227-08.
46. Stabb EV, Reich KA, Ruby EG. 2001. *Vibrio fischeri* genes *hvnA* and *hvnB* encode secreted NAD^+ glycohydrolases. J Bacteriol 183:309–317. https://doi.org/10.1128/JB.183.1.309-317.2001.
47. O'Shea TM, DeLoney-Marino CR, Shibata S, Aizawa S-I, Wolfe AJ, Visick KL. 2005. Magnesium promotes flagellation of *Vibrio fischeri*. J Bacteriol 187:2058–2065. https://doi.org/10.1128/JB.187.6.2058-2065.2005.
48. Lyell NL, Dunn AK, Bose JL, Vescovi SL, Stabb EV. 2008. Effective mutagenesis of *Vibrio fischeri* using hyperactive mini-Tn*5* derivatives. Appl Environ Microbiol 74:7059–7063. https://doi.org/10.1128/AEM.01330-08.
49. Brooks JF, Gyllborg MC, Cronin DC, Quillin SJ, Mallama CA, Foxall R, Whistler C, Goodman AL, Mandel MJ. 2014. Global discovery of colonization determinants in the squid symbiont *Vibrio fischeri*. Proc Natl Acad Sci U S A 111:17284–17289. https://doi.org/10.1073/pnas.1415957111.
50. Visick KL, Skoufos LM. 2001. Two-component sensor required for normal symbiotic colonization of *Euprymna scolopes* by *Vibrio fischeri*. J Bacteriol 183:835–842. https://doi.org/10.1128/JB.183.3.835-842.2001.